# Synthesis, Thermal Stability, and Structure of $(V_{.13}Mo_{.87})O_{2.935}$: A New Oxide with the Open "Hexagonal $MoO_3$" Structure

YATAO HU AND PETER K. DAVIES

*Department of Materials Science and Engineering, University of Pennsylvania 3231 Walnut Street, Philadelphia, Pennsylvania 19104-6272*

New oxides with the stoichiometry $\{Li_xH_{.(3-x)}\}(V_{.13}Mo_{.87})O_3 \cdot 0.26H_2O$ and the structure of "hexagonal $MoO_3$" have been precipitated directly from Li–V–Mo aqueous solutions. At room temperature in dilute HCl, these precipitates undergo a rapid ion-exchange reaction to give the pure protonic form of vanadium-stabilized hexagonal $MoO_3$, $H_{.13}(V_{.13}Mo_{.87})O_3 \cdot 0.26H_2O$. Complete dehydration of this solid acid yields a new oxide $(V_{.13}Mo_{.87})O_{2.935}$ which retains the structure of hexagonal $MoO_3$ up to 460°C. Whereas all the previously reported compounds with the hexagonal $MoO_3$ framework have contained large stabilizing cations in the one dimensional channels of the structure, $(V_{.13}Mo_{.87})O_{2.935}$ represents the open form of hexagonal $MoO_3$ and has empty channels with free diameters approaching 3.3 Å. Powder neutron diffraction was used to confirm the structure of $(V_{.13}Mo_{.87})O_{2.935}$ which was refined in space group $P6_3$ with final lattice parameters of $a = 10.593(1)$, $c = 3.6944(4)$ Å; $V = 359.01$ Å$^3$. The "porosity" of this structure is significantly, $\approx 12$–18%, greater than the $\alpha$, $\beta$, and $\beta'$ polymorphs of $MoO_3$. © 1993 Academic Press, Inc.

## 1. Introduction

In addition to the thermodynamically stable, orthorhombic form of molybdenum trioxide (*1*), $\alpha$-$MoO_3$, two other metastable, $ReO_3$-related, monoclinic polymorphs, $\beta$- and $\beta'$-$MoO_3$, have been prepared using low temperature methods (*2–5*). Over the last twenty years there have also been several reports on the preparation of a hexagonal polymorph of $MoO_3$ (*6–10*). However, two recent papers have shown that these claims are erroneous and that this hexagonal phase corresponds to a partially dehydrated and deammoniated ammonium decamolybdate (*11, 12*). Despite the apparent failure of these methods to produce a new form of $MoO_3$, the open nature (see Fig. 1) and potential application of this hypothetical structure as a catalyst or insertion host has led to increased interest in developing a successful synthetic route to an ammonium-free hexagonal $MoO_3$.

Although the hexagonal polymorph of $MoO_3$ has never been synthesized, a series of closely related compounds containing large stabilizing cations have been reported. In all these structures the molybdate framework consists of zigzag chains of edge-shared octahedra parallel to the $c$ axis; these chains share corners to create large one-dimensional channels, see Fig. 1. The tunnels in the structure are ideally suited to accommodate large alkali metal or ammonium cations which in turn stabilize a series of isomorphous phases. The cations occupying the large tunnel sites can be charge compensated in two ways. In one group of molybdates, with the general stoichiometry $AH_{6x-1}([\square_{Mo}]_xMo_{6-x})O_{18}$ ($x = \frac{2}{3}$ for $A = Na \cdot 2H_2O$, $Ag \cdot 2H_2O$, K, Rb, Cs, and $NH_4$ by MaCarron et al. (*11*); $x = 1$ for $A = K$ by Krebs and Paulat-Boschen (*12*); and $x = 1$ for $NH_4$ by Caiger et al. (*13*), $\square_{Mo}$ represents a molybdenum vacancy), the charge of the large stabilizing cations in the tunnels
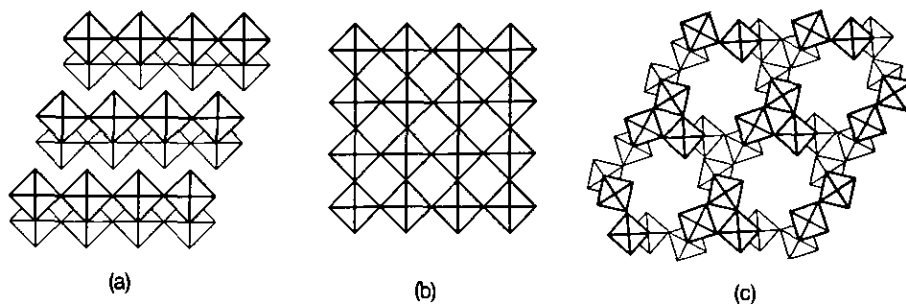
FIG. 1. Idealized projections of (a) $\alpha$-MoO$_3$, (b) $\beta$- and $\beta'$-MoO$_3$, and (c) hexagonal MoO$_3$.

is compensated by molybdenum vacancies in the framework. This class of compounds is prepared by precipitation from acidified molybdate solutions. In the second group of hexagonal phases the charge of the large cations occupying the channel sites is compensated by the partial substitution of vanadium into the framework. The vanadium-stabilized structures, $A_x(V_xMo_{1-x})O_3$ ($A =$ K, NH$_4$, Rb, Cs), can be prepared by a standard solid state method and occur for only a narrow range of $x$; $0.11 < x < 0.14$ (14, 15).

The previous attempts to synthesize an "open" form of hexagonal MoO$_3$ with empty channels, have focused on the deammoniation reactions of $(NH_4)H_{6x-1}(\square_{Mo})_x$ $Mo_{6-x}O_{18}(x = \frac{2}{3}, 1)$. Although partial deammoniation proceeds without any major structural rearrangements, the hexagonal ammonium molybdates were found to undergo bulk decomposition prior to the completion of the deammoniation reaction (11, 12). Following from that work it was suggested that the presence of the large cations in the tunnels is essential to the stabilization of this hexagonal structure (11, 12). However, very recently in this laboratory we demonstrated that the open V-stabilized form of hexagonal MoO$_3$, $(V_{.13}Mo_{.87})O_{2.935}$, could be prepared by the dehydration of a protonic hexagonal molybdate, $H_{.13}(V_{.13}Mo_{.87})O_3 \cdot 0.26H_2O$ (16, 17). This new protonic precursor to the open hexagonal form of MoO$_3$, was formed by a novel partial solvolysis or leaching reaction be-

tween lithium brannerite (LiVMoO$_6$) and dilute hydrochloric acid solutions.

Although the unusual reactions of LiV MoO$_6$ in aqueous acids provide a successful route to the formation of the open hexagonal MoO$_3$ structure, the yields of H$_{.13}$ $(V_{.13}Mo_{.87})O_3 \cdot 0.26H_2O$ can be fairly low. This is primarily due to the simultaneous formation of small quantities of an amorphous phase that must be removed from the product by a subsequent wash in stronger acids. To fully investigate the structure and properties of this new form of vanadium-stabilized MoO$_3$ we have explored alternative routes for the preparation of bulk quantities of the protonic hexagonal MoO$_3$ precursor. In this paper we present a method for the synthesis of $H_{.13}(V_{.13}Mo_{.87})$ $O_3 \cdot 0.26H_2O$, involving direct precipitation from aqueous lithium vanadium molybdate solutions and subsequent ion-exchange reaction in dilute HCl solution. In particular we have examined the effect of the parameters that control the formation of the hexagonal MoO$_3$ precipitates, including the composition, pH and temperature of the acidic solutions. We also present new results on the stability and structure of the open hexagonal $(V_{.13}Mo_{.87})O_{2.935}$ phase using thermal analysis and powder neutron diffraction.

## 2. Synthesis Procedure and Experimental Techniques

The goal of this work was to develop a route to directly precipitate an isomorph of

vanadium-stabilized hexagonal $MoO_3$ that could be easily converted to the open $(V_{.13}Mo_{.87})O_{2.935}$ phase by chimie douce methods. Previous studies on the pure molybdate hexagonal phases and additional experiments in this laboratory on the vanadium-stabilized phases, indicated that direct thermolysis of the ammonium isomorphs lead to bulk decomposition of the hexagonal structure prior to complete deammoniation. However, from our studies of the reactions of the alkali brannerites, $AV$ $MoO_6$ $(A = Li, Na, K)$, it was apparent that the hydronium form of hexagonal $MoO_3$, $H_{.13}(V_{.13}Mo_{.87})O_3 \cdot 0.26H_2O$, could be completely dehydrated to the open $(V_{.13}Mo_{.87})$ $O_{2.935}$ phase without inducing the bulk decomposition and collapse of the hexagonal framework. Therefore, one of the challenges in successfully stabilizing the open hexagonal phase lies in preparing a hexagonal precursor that can be completely converted into $H_{.13}(V_{.13}Mo_{.87})O_3 \cdot 0.26H_2O$. Perhaps the most obvious method for the preparation of the protonic precursor is through a simple ion-exchange reaction of either the ammonium or alkali hexagonal $A_{.13}(V_{.13}Mo_{.87})O_3 \cdot 0.26H_2O$ phases. However, for the hexagonal vanadium molybdates with $A = Na$, $NH_4$ and $K$, extended ion exchanges in HCl solutions with a range of acid strengths resulted in either no observable ion exchange or in bulk decomposition to unrelated phases via partial or complete dissolution reactions. The only cation stabilized hexagonal molybdate that was found to participate in a proton exchange reaction was the Li-containing isomorph formed from the partial solvolysis reaction of lithium brannerite $(LiVMoO_6)$. It was for this reason that our precipitation reactions focused on the products formed upon the acidification of Li–V–Mo aqueous solutions.

Two approaches were designed to directly precipitate samples of the lithium–hydronium isomorphs of vanadium stabilized hexagonal $MoO_3$. In the first, approach A, $V_2O_5$ and $\alpha$-$MoO_3$ with the desired V : Mo

content were dissolved in 1.0 $M$ LiOH such that $[V + Mo] = 0.33$ $M$, the solution was then acidified by the addition of 1.0 M HCl. The addition of HCl was monitored by a pH meter (Orion SA720) and stopped when the desired pH was obtained; the acidified solution was then refluxed at temperatures ranging from 60 to 90°C for 16 hr. No attempt was made to further control the pH of the solution during the reaction. In the second, approach B, $LiVO_3$ and $Li_2Mo_2O_7$ (prepared by conventional solid state reaction) with the desired V : Mo content were dissolved in water such that $[V + Mo] = 0.17 M$, and the solution was again acidified and refluxed under the same conditions. The precipitates from these solutions were collected by vacuum filtration and dried in a desiccator. Because of the limited solubility of $V_2O_5$ and $MoO_3$, using approach B it was possible to investigate the nature of the precipitates from solutions with much lower relative Li concentrations $([Li] : [V + Mo] = 3 : 1$ for approach A and 1 : 1 for approach B). The concentrations of $(V + Mo)$ of the solutions by both approaches prior to acidification were chosen so that they were the same after the solutions been acidified to pH = 1.0.

Phase identification of the precipitates from these solutions was carried out by powder x-ray diffraction (XRD) using a Rigaku DMAX-B diffractometer and $CuK\alpha$ radiation. The morphology of the precipitates was examined using scanning electron microscopy (SEM). Atomic absorption (AA) was used for compositional analyses; thermogravimetric analysis (TGA, DuPont TGA951) and differential scanning calorimetry (DSC, SETARAM DSC111) were employed to investigate the thermal stability.

Structure determinations of $(V_{.13}Mo_{.87})$ $O_{2.935}$ were conducted by powder neutron diffraction refinement using the Rietveld technique. The neutron diffraction data were collected using the triple-axis spectrometer on the H4S beamline at the High Flux Beam Reactor (HFBR) at Brookhaven National Laboratory. A Si (400) incident

beam monochromator was used to provide a neutron beam with a wavelength of 1.358 Å. The powder samples of $(V_{.13}Mo_{.87})O_{2.935}$ were sealed in an aluminum container under $N_2$ gas. Data were collected at room temperature from 5 to 120° in 0.1° steps.

## 3. Results and Discussion

### 3.1 Solution Synthesis

Direct precipitation methods have been used (11, 12) to prepare the Na and $NH_4$ salts of hexagonal $MoO_3$ (hereafter designated as h-$MoO_3$); as described earlier, neither of these isomorphs can be used as precursors to the open form of the hexagonal structure. Following our work on the successful formation of the open structure from the partial solvolysis reactions of lithium brannerite, we focused on the direct precipitation of vanadium-stabilized h-$MoO_3$ from acidified Li–V–Mo solutions. It is well known that the structures of the complex polyanion solution clusters in the vanadate–molybdate solutions strongly depend upon the composition of the solution (especially the V : Mo concentration and the nature and concentration of the alkali metal ions), the pH of the solution, and the reaction temperature. In this regard the Li–V–Mo system is no exception, and the crystallography of the precipitates, and by inference the structure of the polyanions, was highly sensitive to the relative concentrations of the dissolved cations, the pH, and the reflux temperature. As described below, although it was possible to directly precipitate h-$MoO_3$ from these solutions, the window of stability for this phase is extremely narrow.

(a) Effect of the [V] : [Mo] concentration in solution. Approach A was used to prepare solutions with V : Mo = 0.13 : 0.87; 0.15 : 0.85; and 0.20 : 0.80, which were acidified to pH = 1.0 and refluxed at 80°C for 16 hr (the effect of changes in the initial pH of the solution and temperature are discussed below). The X-ray diffraction pat-



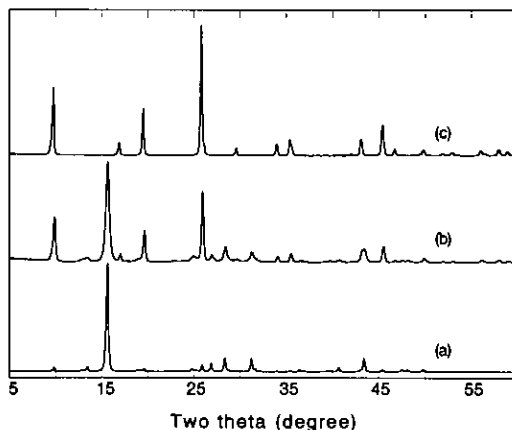FIG. 2. X-ray diffraction patterns of the solid precipitates collected from Li–V–Mo solutions with pH = 1 and V : Mo = (a) 0.13 : 0.87, (b) 0.15 : 0.85, and (c) 0.20 : 0.80. Solutions were prepared using approach A and refluxed at 80°C.

terns collected from the solid precipitates are presented in Fig. 2. Using a V : Mo solution concentration = 0.13 : 0.87, the same relative concentration as that in V-stabilized h-$MoO_3$, the precipitate was hydrated α-$MoO_3$ ($MoO_3 \cdot H_2O$), together with trace amounts of $MoO_3 \cdot 0.5H_2O$ and h-$MoO_3$. For V : Mo = 0.15 : 0.85, both $MoO_3 \cdot H_2O$ and h-$MoO_3$ are present in the precipitate; however, when the concentration of V : Mo reaches 0.2 : 0.8 the well crystallized yellow precipitate is comprised of a single phase of vanadium-stabilized h-$MoO_3$. Continued increases in the concentration of vanadium in solution result in the formation of an additional amorphous phase believed to be $V_2O_5$, see below.

(b) Effect of [Li] in solution. The structure of the precipitates was also found to be highly sensitive to the relative concentrations of Li in the acidic solutions. By using approaches A and B it was possible to study this effect over a significant range of Li concentrations. For solutions prepared using approach A, the minimization of [Li] is limited by the solubility of $V_2O_5$ and $MoO_3$ in the basic solution. The typical ratio of the concentration of Li to that of the transition
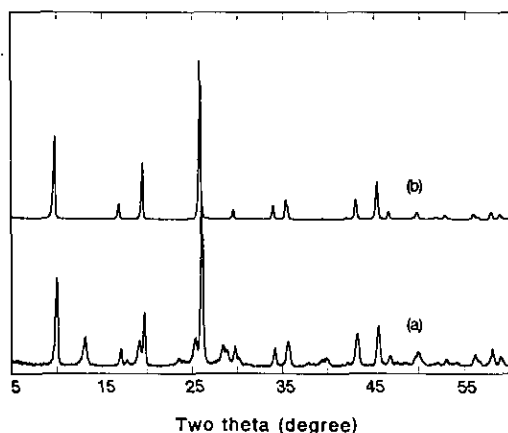
FIG. 3. X-ray diffraction patterns of the precipitates from solutions at with V : Mo = 0.20 : 0.80, pH = 1, $T = 80°C$, and [Li] = (a) 0.13 $M$ and (b) 0.4 $M$. Solutions were prepared using approach B, for (b) LiCl was added to raise [Li].

metal ions (V + Mo) is about 3 : 1. Using approach B, in which $LiVO_3$ and $Li_2Mo_2O_7$ were dissolved in $H_2O$, the concentration of Li in solution can be reduced to [Li] : [V + Mo] = 1 : 1.

Figure 3a shows the X-ray diffraction pattern of a solid precipitated from a solution with V : Mo = 0.2 : 0.8 and a pH = 1.0 prepared using approach B. This solid was identified as a mixture of h-MoO$_3$ and hydrated molybdenum trioxides. In contrast, solutions with the same V : Mo concentration and pH that were prepared using approach A yielded a pure, single phase h-MoO$_3$ precipitate. The only obvious difference between these two solutions was the concentration of Li. The concentration of Li in the solution prepared by method B was increased to 0.4 $M$ through the addition of LiCl, which is the typical concentration of Li for solutions prepared using approach A after acidification. After reaction at 80°C this solution produced a single phase of h-MoO$_3$, as indicated by the X-ray diffraction pattern shown in Fig. 3b. For solutions prepared using approach B with pH = 1.0, single phase samples of h-MoO$_3$ can only be produced by raising the V : Mo content to ≈0.33 : 0.67.

(c) *Effect of pH.* To investigate how the pH of the solutions changes the precipitated phases, solutions with Li : V : Mo = 3.0 : 0.20 : 0.80 were refluxed at 80°C at several different pH values. For a pH between 2 and 5 there was no evidence of any solid precipitate even after one week of reaction at 80°C. X-ray diffraction patterns of the precipitates collected from solutions with a pH = 0.75–1.5 are shown in Fig. 4. At pH = 0.75, the solid phase was identified as $MoO_3 \cdot 0.5H_2O$. When the value of pH is increased to 0.85, the precipitate was a mixture of $MoO_3 \cdot 0.5H_2O$ and h-MoO$_3$, whereas for a pH = 1 a single phase sample of h-MoO$_3$ was formed. At higher pH values, for example 1.5, a brown precipitate was formed and X-ray diffraction showed that this solid was a two-phase mixture of h-MoO$_3$ and an amorphous material characterized by a broad diffraction peak between 5 and 8° 2θ. It should be recalled that this amorphous phase was also observed as an intermediate product during formation of h-MoO$_3$ via the leaching reaction of lithium brannerite (LiVMoO$_6$) (*16, 17*). The amorphous phase is unstable at lower pH's and can be readily dissolved by reimmersing the as-precipitated, two-phase-mixture in 0.5 $M$
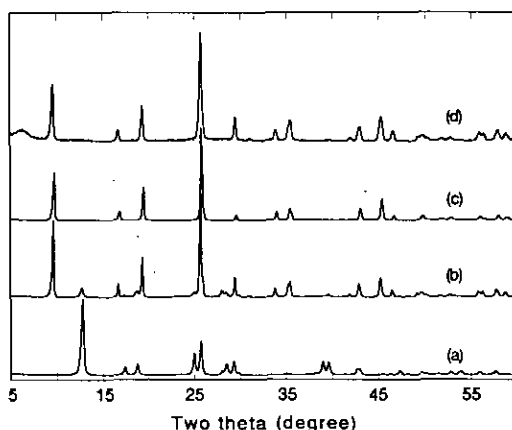


FIG. 4. X-ray diffraction patterns of the solids precipitated from solutions at 80°C with V : Mo = 0.20 : 0.80 and pH = (a) 0.75, (b) 0.85, (c) 1.0, and (d) 1.5. Solutions were prepared using approach A.
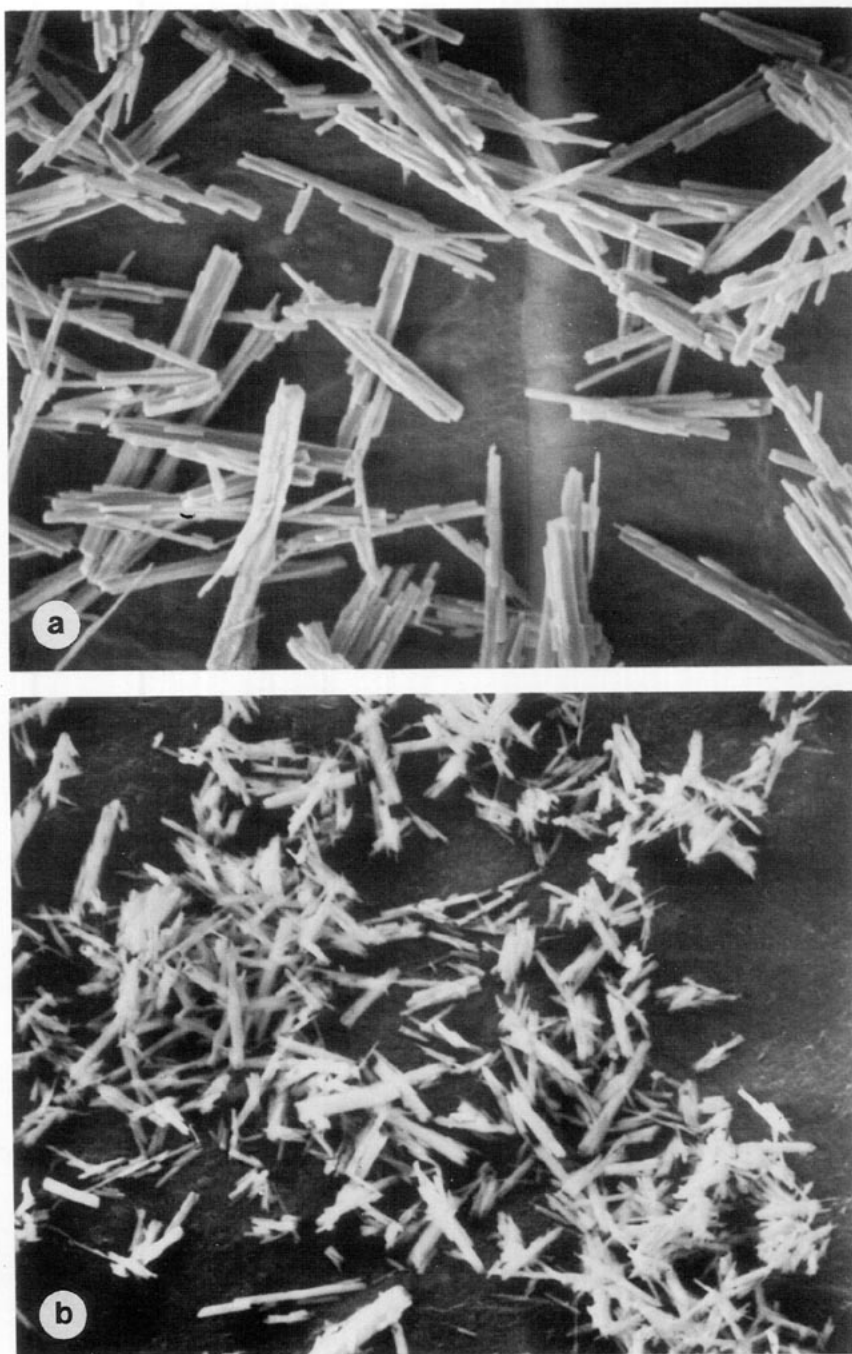
FIG. 5. SEM micrographs of the hexagonal $MoO_3$ precipitates formed from solutions with $V : Mo = 0.20 : 0.80$, pH $= 1$ and $T = $ (a) 75 and (b) 90°C. Solutions were prepared using approach A. (c) h-$MoO_3$ prepared by the leaching reaction of $LiVMoO_6$. Marker $= 10 \ \mu$m.
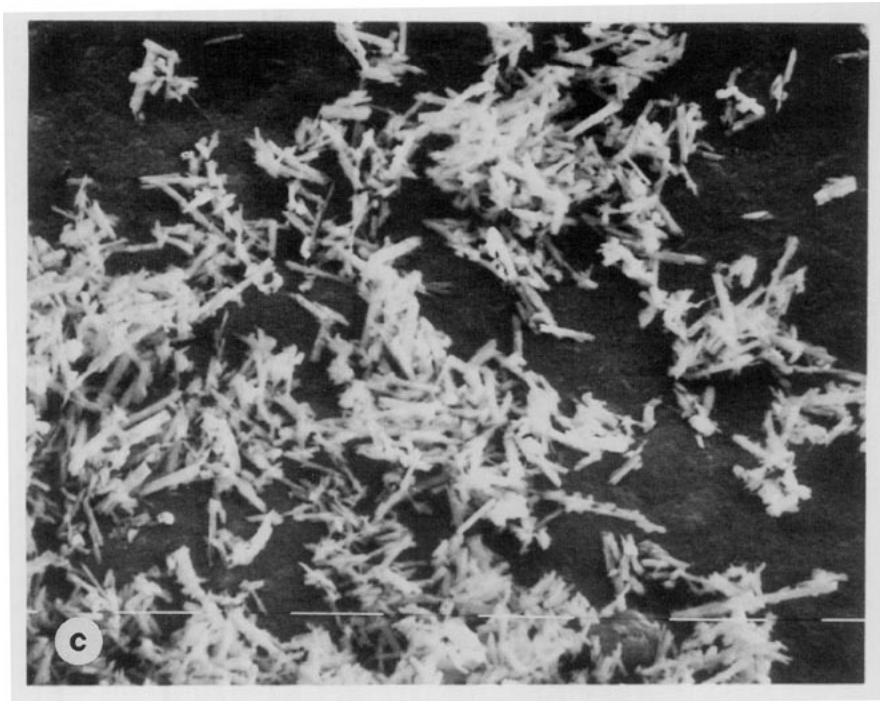
FIG. 5—*Continued*

HCl at room temperature for 1 or 2 hr. Energy dispersive X-ray analyses of the solids before and after acid washing indicated that the amorphous material was vanadium-rich and is most probably a hydrated $V_2O_5$ precipitate (*18*). The presence of this amorphous material in the precipitates from solutions with a higher value of pH (1.5), but not in those with a lower pH (1.0), is consistent with the expected increase in the solubility of vanadium in solutions with higher acidities.

(*d*) *Effect of reflux temperature*. The effect of temperature on the stabilities of the precipitates was examined by refluxing solutions prepared using method A with V : Mo = 0.2 : 0.8 and pH = 1.0 at 60, 75, and 90°C. At 60°C, a slow precipitation reaction yielded pure hydrated molybdenum trioxide; single phase samples of h-MoO₃ could only be obtained by raising the temperature to 75°C and above. The reaction temperature also had a significant effect upon the crystallite size of the precipitates.

In Fig. 5 we show SEM micrographs of the h-MoO₃ products collected from these two temperatures. In both cases, h-MoO₃ crystallizes in the form of needles with particle sizes of 10–35 × 1–3 $\mu$m for the 75°C sample, and 5–10 × 0.5–1 $\mu$m for the case of 90°C. The $c$ axis of the hexagonal phase corresponds to the longer direction. The decrease in the size of the crystallites with increasing temperature was utilized in the preparation of samples for subsequent investigations of the ion-exchange and ion-insertion properties. It is interesting to compare the morphology of these solution precipitates to the hexagonal phases produced by the leaching reaction of lithium brannerite which is conducted at 60°C, see Fig. 5c. In this case the average size of the particles is about 3–5 × 0.5–1 $\mu$m; this is somewhat smaller than those produced by any of the direct precipitation reactions.

The results described above indicate that h-MoO₃ has a very limited stability in Li–V–Mo aqueous solutions. In summary,

TABLE I

COMPOSITIONS OF h-MoO$_3$
{Li$_x$H$_{.13-x}$}(V$_{.13}$Mo$_{.87}$)O$_3 \cdot 0.26$H$_2$O SAMPLES

| Sample | Sample description | $x$ |
|--------|-------------------|-----|
| 1 | As-precipitated h-MoO$_3$ from solution prepared using approach A and with V : Mo = 0.2 : 0.8 | 0.085 |
| 2 | Sample 1 exchanged in 0.5 $M$ HCl | 0.003 |
| 3 | As-precipitated h-MoO$_3$ from solution prepared using approach B and with V : Mo = 0.33 : 0.67 | 0.009 |
| 4 | Sample exchanged in 0.5 $M$ HCl | 0.003 |

the maximum yields of single-phase h-MoO$_3$ precipitates could be prepared from solutions of V$_2$O$_5$ and $\alpha$-MoO$_3$ in 1.0 $M$ LiOH, with [V + Mo] = 0.33 $M$ and [V] : [Mo] = 0.2 : 0.8, by lowering the pH to 1.0 through the addition of HCl and then refluxing at 80°C for approximately 16 hr.

(e) *Compositions of the hexagonal MoO$_3$ precipitates.* Although the nature of the phases precipitated from the Li–V–Mo solutions are highly dependent upon the relative concentrations of the solvated ions, pH and temperature, chemical analyses indicate that the relative vanadium to molybdenum content of all the h-MoO$_3$ precipitates remains constant at 0.13 : 0.87. This is in contrast to the corresponding Na–V–Mo system, in which the vanadium content of the hexagonal structure can be continuously varied from 0.13 to 0.0 (*19*). Although the composition of the framework is independent of that of the solution, the composition of the ions in the channels of the hexagonal structure is highly dependent upon the relative concentration of Li in solution. The general stoichiometry of all of the hexagonal precipitates can be expressed as {Li$_x$H$_{.13-x}$}(V$_{.13}$Mo$_{.87}$)O$_3 \cdot 0.26$H$_2$O, with the exact value of $x$ being determined by the concentration of Li in solution, see Table I. For example, solutions prepared using approach A with Li : V : Mo = 3.0 : 0.2 : 0.8 and

pH = 1.0, yielded a phase with $x$ = 0.085, i.e., {Li$_{.085}$H$_{.045}$}(V$_{.13}$Mo$_{.87}$)O$_3 \cdot$ 0.26H$_2$O; the precipitates from solutions prepared using approach B, with Li : V : Mo = 1.0 : 0.33 : 0.67 and pH = 1.0, have a stoichiometry of {Li$_{.009}$H$_{.121}$}(V$_{.13}$Mo$_{.87}$)O$_3 \cdot$ 0.26H$_2$O.

The variability in the Li content of these samples can be utilized to prepare both the pure protonic form of h-MoO$_3$ as well as the pure lithium isomorph. The protonic form, H$_{.13}$(V$_{.13}$Mo$_{.87}$)O$_3 \cdot 0.26$H$_2$O was readily obtained by ion-exchanging the precipitates in 0.5 $M$ HCl (1 g/50 ml) at room temperature. The precipitates from different solutions, i.e., with different initial Li contents, could all be completely exchanged to this pure protonic product in less than 2 hr. However, it should be noted that prolonged exposure at elevated temperature leads to bulk decomposition and formation of hydrated $\alpha$-MoO$_3$. The chemical composition of the ion-exchanged products was confirmed by atomic absorption analysis. It was also possible to prepare the pure lithium isomorph, Li$_{.13}$ (V$_{.13}$Mo$_{.87}$)O$_3 \cdot 0.26$H$_2$O, by ion-exchanging the precipitates in aqueous LiCl solutions at 60°C. The synthesis, thermal stability, and structures of those systems will be described elsewhere.

## 3.2 Preparation and Thermal Stability of (V$_{.13}$Mo$_{.87}$)O$_{2.935}$

As reported previously for the leaching reactions of lithium brannerite (*16, 17*), the open form of V-stabilized h-MoO$_3$ was readily obtained by the low temperature thermolysis of H$_{.13}$(V$_{.13}$Mo$_{.87}$)O$_3 \cdot 0.26$H$_2$O. In Fig. 6 we present the results of TGA and DSC scans of the samples of H$_{.13}$(V$_{.13}$Mo$_{.87}$)O$_3 \cdot 0.26$H$_2$O prepared via the direct precipitation reactions. For both scans, the samples were heated at 5°C/min in a flow of helium gas. Besides the loss of surface water, two discrete weight losses are expected for H$_{.13}$(V$_{.13}$Mo$_{.87}$)O$_3 \cdot 0.26$H$_2$O
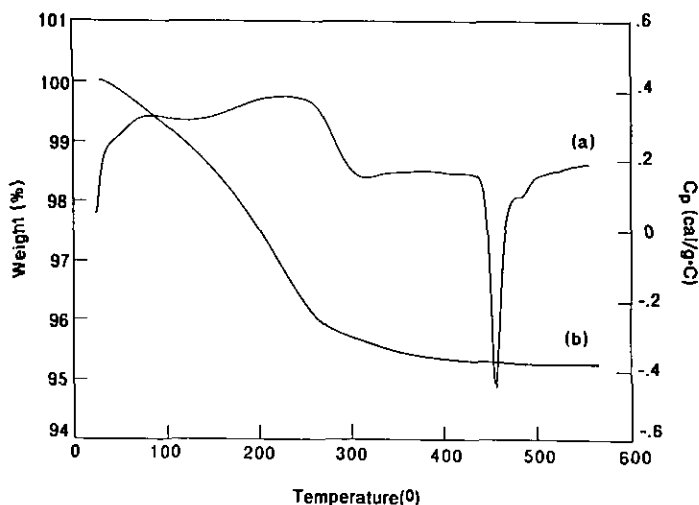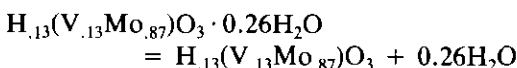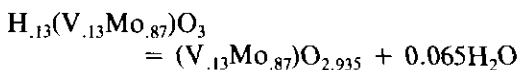
FIG. 6. (a) DSC and (b) TGA scans of $H_{.13}(V_{.13}Mo_{.87})O_3 \cdot 0.26H_2O$. Heating rate is 5°C/min.

according to

$$H_{.13}(V_{.13}Mo_{.87})O_3 \cdot 0.26H_2O$$
$$= H_{.13}(V_{.13}Mo_{.87})O_3 + 0.26H_2O$$

and

$$H_{.13}(V_{.13}Mo_{.87})O_3$$
$$= (V_{.13}Mo_{.87})O_{2.935} + 0.065H_2O$$

The TGA, lower curve in Fig. 6, indicates that under the heating rate of 5°C/min, all weight losses are complete below 350°C. The first weight loss, which corresponds to the removal of the 0.26 moles of water of hydration presumably located in the channels of the structure, occurs between approximately 100 and 250°C. The second weight loss, which corresponds to the removal of the protons and a small fraction of associated framework oxygen atoms, occurs between 250 and 350°C. The final product of these dehydration reactions has a yellow-greenish color and the nominal stoichiometry, $(V_{.13}Mo_{.87})O_{2.935}$. Powder X-ray diffraction indicates that this compound retains the h-MoO₃ tunnel structure and thermal analysis by DSC, upper curve in Fig. 6, shows that it is stable up to 460°C.

The main structure feature of $(V_{.13}Mo_{.87})$ $O_{2.935}$ that distinguishes it from all the other h-MoO₃ isomorphs is the absence of any

large, "stabilizing" cations in the one-dimensional channels. There have been several attempts to stabilize this open form of hexagonal MoO₃. These have primarily focused on the deammoniation reactions of the vacancy-stabilized ammonium isomorphs of h-MoO₃, i.e., $(NH_4)H_{6x-1}Mo_{6-x}O_{18}(x = \frac{2}{3}, 1)$ (11, 12). In this case the formation of the open structure was thwarted by the premature bulk decomposition of the hexagonal framework prior to the final deammoniation reaction. In an investigation of the thermal stability of $(NH_4)_{.13}(V_{.13}Mo_{.87})O_3 \cdot nH_2O$ prepared by ion-exchange reaction, our experimental results show that the deammoniation reaction proceeds in several steps, see Fig. 7, with the final weight loss occurring at approximately 490°C under a heating rate of 5°C/min. Because this final reaction occurs 30°C higher than the upper stability limit of the open form of vanadium-stabilized h-MoO₃, it is apparent that $(V_{.13}Mo_{.87})O_{2.935}$ also cannot be formed by a direct deammoniation reaction. Although we have not been able to form the pure molybdate form of h-MoO₃, it is likely that the Mo vacancies in the framework would further reduce the upper stability limit; again this is confirmed by the collapse of the structure during the deam-
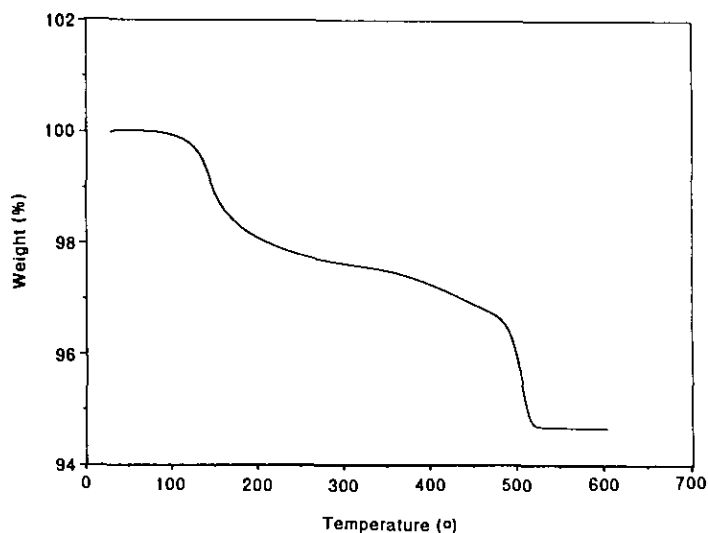
FIG. 7. TGA scan of $(NH_4)_{.13}(V_{.13}Mo_{.87})O_3 \cdot nH_2O$.

moniation reactions of $(NH_4)H_{6x-1}(\square_{Mo})_x$ $Mo_{6-x}O_{18}(x = \frac{2}{3}, x = 1)$ (*11, 12*).

### 3.3 Structure Determination of $(V_{.13}Mo_{.87})O_{2.935}$

The structure of the open form of vanadium stabilized h-$MoO_3$ was investigated using powder neutron diffraction. Approximately 6 g $(V_{.13}Mo_{.87})O_{2.935}$ were prepared by heating samples of $H_{.13}(V_{.13}Mo_{.87})O_3 \cdot$ $0.26H_2O$ at 350°C for 16 hr. Because $(V_{.13}Mo_{.87})O_{2.935}$ slowly rehydrates if it is exposed to atmospheric water, the heating and cooling of the sample was carried out under a dry flow of argon gas. The sample was sealed in an aluminum container under dried $N_2$ gas. The diffraction data were collected at room temperature from 5 to 120° in 0.1° steps and the diffraction profiles were analyzed using the Rietveld technique. Because some reflections from $(V_{.13}Mo_{.87})O_{2.935}$ and the aluminum container overlapped, the final data analysis was conducted by refining these two phases simultaneously. The structure of $(V_{.13}Mo_{.87})O_{2.935}$ was solved in space group $P6_3$ using a refined cell with $a =$ 10.593(1), $c = 3.6944(4)$ Å and $V = 359.01$ Å$^3$. During the refinement, a Pseudo-Voigt peak profile function was used and the fol-

lowing parameters were refined: zero-point, background parameters, scale factors, lattice parameters, FWHM parameters, peak profile parameters, peak asymmetry parameter, atomic coordinates, isotropic temperature factors, preferred orientation, and occupancies. No anisotropic temperature factor refinement was attempted. The final values of the agreement indices for the refinement were $R_p = 0.078$, $R_{wp} = 0.109$, and $R_B = 0.05$ with a GOF = 1.4.

Figure 8 shows the observed diffraction pattern (+), the calculated pattern (solid line), and their difference profile. The upper set of bars indicate the position of reflections from $(V_{.13}Mo_{.87})O_{2.935}$, while the lower set of bars indicate the position of the reflections from Al. In Table II we list the refined atomic positions, the isotropic temperature factors, and the site occupancies. As expected the overall features of the structure of $(V_{.13}Mo_{.87})O_{2.935}$ are very similar to those of the hexagonal compound, $K_{.13}(V_{.13}Mo_{.87})O_3$ which was originally refined using single crystal X-ray techniques by Darriet and Galy (*14*). Difference Fourier maps showed no evidence of any species in the tunnels and confirmed the open nature of this form of V-stabilized h-$MoO_3$. The
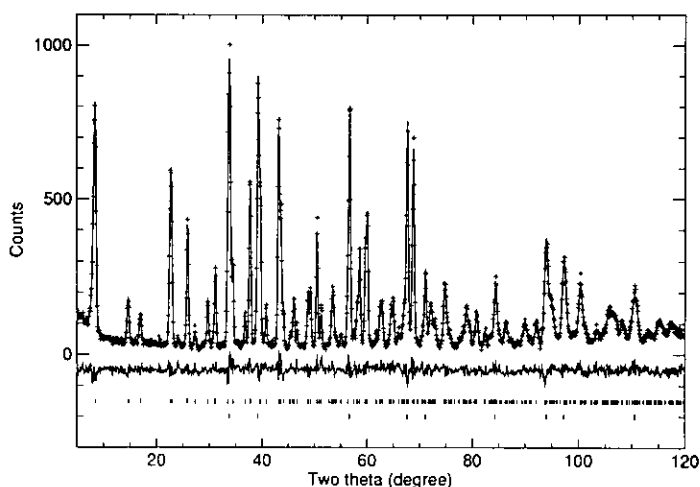
FIG. 8. Observed (+), calculated (solid line) neutron diffraction patterns, and their difference for $(V_{.13}Mo_{.87})O_{2.935}$. The upper set of bars indicates the position of reflections from $(V_{.13}Mo_{.87})O_{2.935}$, and the lower set of bars indicates the positions of reflections from the aluminum container.

TABLE II

REFINED ATOMIC COORDINATES, ISOTROPIC TEMPERATURE FACTORS, AND SITE OCCUPANCIES
FOR $(V_{.13}Mo_{.87})O_{2.935}$

| Atom | Site | $x$ | $y$ | $z$ | $B(\text{Å}^2)$ | Occu. |
|------|------|-----|-----|-----|------|-------|
| V    | 6c   | 0.3520(4) | 0.4573(4) | 0.72(1)  | 0.56(8) | 0.12(1)  |
| Mo   | 6c   | 0.3520(4) | 0.4573(4) | 0.72(1)  | 0.56(8) | 0.88(1)  |
| O(1) | 6c   | 0.2648(5) | 0.2746(5) | 0.73(1)  | 1.6(1)  | 0.940(5) |
| O2   | 6c   | 0.2158(5) | 0.4987(6) | 0.70(1)  | 1.0(1)  | 1.00     |
| O3   | 6c   | 0.4202(5) | 0.4992(5) | 0.215(7) | 0.65(9) | 1.00     |

*Note.* $a = 10.593(1)$, $c = 3.6994(4)$ Å, $R_p = 7.8\%$, $R_{wp} = 10.9\%$, $R_B = 5.0\%$, GOF $= 1.4$.

$$R_p = \frac{\sum |y_{io} - y_{ic}|}{\sum y_{ic}}$$

$$R_{wp} = \left[\frac{\sum w_i(y_{io} - y_{ic})^2}{\sum w_i y_{io}^2}\right]$$

$$R_B = \frac{\sum |I_{ko} - I_{kc}|}{\sum I_{ko}}$$

$$\text{GOF} = \frac{\sum w_i(y_{io} - y_{ic})^2}{N - P}$$

$N$ = number of independent observations, $P$ = number of parameters, $y$ = counts, $I$ = integrated Bragg intensities, and $w$ = weights.

HU AND DAVIES

TABLE III

SELECTED INTERATOMIC DISTANCES (Å) AND ANGLES (°) FOR $(V_{.13}Mo_{.87})O_{2.935}$

| | | | |
|---|---|---|---|
| $M$ | $-M$ | 3.35 | $O(1)-M-O(2)$ 104.4 |
| | $-O(1)$ | 1.68 | $O(1)-M-O(3)$ 98.9, 99.9, 102.1 |
| | $-O(2)$ | 1.71, 2.39 | $O(2)-M-O(2)$ 82.0 |
| | $-O(3)$ | 1.93, 1.97, 2.22 | $O(2)-M-O(3)$ 74.7, 75.7, 79.0, 99.4, 104.4 |
| $O(1)$ | $-O(1)$ | 3.40 | $O(3)-M-O(3)$ 73.0, 73.6 |
| | $-O(2)$ | 2.67, 2.99, 3.12 | |
| | $-O(3)$ | 2.77, 2.84, 2.98 | |
| $O(2)$ | $-O(2)$ | 2.74 | |
| | $-O(3)$ | 2.70, 2.78, 2.80, 2.88 | |
| $O(3)$ | $-O(3)$ | 2.50 | |

*Note.* ($M$ = Mo or V).

framework of the structure consists of zig-zag chains of edge-shared octahedra parallel to the $c$ axis, these chains share corners to create large one-dimensional tunnels. Although the structure can be described in terms of corner- and edge-shared Mo octahedra, the actual coordination polyhedra are significantly distorted. Table III lists some interatomic distances and bond angles for $(V_{.13}Mo_{.87})O_{2.935}$. Based on these data, the $MO_6$ ($M$ = V, Mo) octahedron is schematically drawn in Fig. 9, with the corresponding bond lengths indicated. As expected the
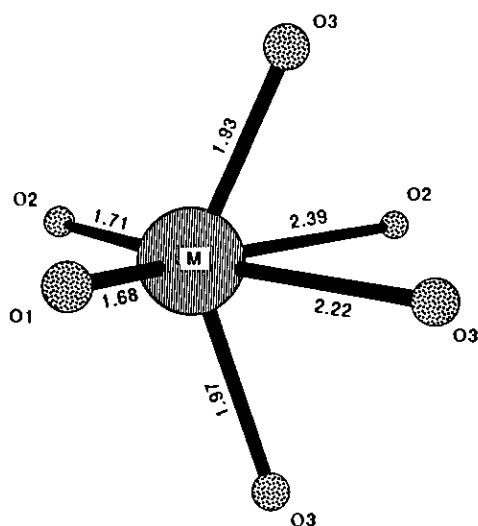


FIG. 9. Schematic representation of the distorted $MO_6$ ($M$ = V, Mo) octahedron in h-$(V_{.13}Mo_{.87})O_{2.935}$.

$MO_6$ octahedron is heavily distorted and the Mo–O bond lengths (1.68, 1.71; 1.93, 1.97; 2.22, 2.39 Å) indicate that the 2 + 2 + 2 type coordination is very similar to that observed for $\alpha$-MoO$_3$ and many other molybdates. In this structure the MoO$_6$ octahedron is distorted in such a way as to maximize the distance between the transition metal framework atoms.

The channels in the h-MoO$_3$ structure are bounded by six corner-shared octahedra and six edge-sharing octahedra, this results in a tunnel diameter that is significantly larger than that in the corresponding hexagonal WO$_3$ structures where the channels are formed from six corner-shared octahedra (20), see Fig. 10. The different framework arrangements in these two structure types lead to a range of different types of oxygen anions at the perimeter of the channels. Whereas all the surrounding anions in hexagonal WO$_3$ are corner shared, in h-MoO$_3$ there are three different coordination sites for oxygen. One-third of the oxygens (O(1)) are bonded to a single framework cation, one-third (O(2)) are corner-shared between two cations with the remaining one-third (O(3)) being bonded to three cations in the framework. The refined site occupancies of the framework are in excellent agreement with those expected from the chemical analyses of the cation concentrations and with the oxygen content of the lattice deduced from the thermal analyses. As shown in Ta-
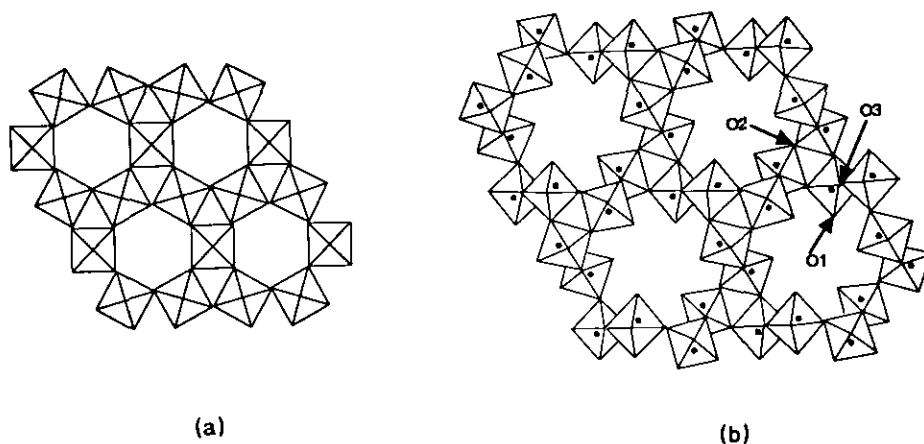
(a)

(b)

FIG. 10. (a) idealized structure of hexagonal $WO_3$; (b) refined Mo positions in hexagonal $(V_{.13}Mo_{.87})O_{2.935}$.

ble III, the vanadium to molybdenum concentration is within one standard deviation of the chemically determined ratio of 0.13 : 0.87, and the total oxygen content also freely refined to 2.94. The refinement shows that the anion vacancies exclusively populate the O(1) sites which correspond to the unshared oxygen positions in the framework. The O(1) position is the most basic oxygen ion in the structure and is the most likely site for the protons in the $H_{.13}$ $(V_{.13}Mo_{.87})O_3 \cdot 0.26H_2O$ acidic precursor to the open hexagonal structure. Therefore, it seems logical that the oxygen ions lost during the preparation of $(V_{.13}Mo_{.87})O_{2.935}$ are removed from the unshared O(1) position. It is also reasonable to believe that these vacant O(1) sites are associated with the V ions, which readily accept fivefold coordination, in the framework as opposed to Mo.

The iostropic temperature factors for the O(1), O(2), and O(3) sites are 1.60, 1.0, and 0.65, respectively. Because the isotropic temperature factors are proportional to $\langle u^2 \rangle$, the mean square displacement of the atom due to thermal vibration, these should directly reflect the strength of the bond between each atom and the framework. Again the observed trend is in good agreement with that expected on simple crystal chemical grounds. The O(1) atoms, with the largest thermal factor, are bonded to one Mo(V) atom, the atoms occupying the O(3) site are coordinated to three framework cations and have the lowest thermal factor; the thermal factor for the doubly coordinate O(2) site lies in between these two.

The atom positions obtained from the structure refinement were used to calculate the bond strengths in the open $(V_{.13}Mo_{.87})$ $O_{2.935}$ structure using the bond valence methods developed by Brown (21) and modified by Brese and O'Keeffe (22) for operation on a Macintosh PC (EUTAX). The final bond strengths were calculated from a compositionally weighted average (0.87 : 0.13) of those obtained for a pure Mo and pure V framework, see Table IV. The valence sums for each atom are in good agreement with those predicted by the chemical stoichiometry and support the validity of the refined atom positions. For example, at the framework cation site the valence sum is 5.86 (c.f. 5.87) and the low valence sum at the O(1) site, 1.803, is consistent with the expected and refined occupancy, $0.935 \times 2 = 1.87$.

The main feature of this form of $h$-$MoO_3$ is the absence of any larger cations in the tunnel positions. According to the refinement, the distance from O(1) to O(1) measured across the diameter of the tunnels is 6.01 Å. This implies a free diameter within

### TABLE IV

Bond Strengths in $(V_{.13}Mo_{.87})O_{2.935}$

| Atom | Distance (Å) | Bond strength (valence units) | Valence sum |
|---|---|---|---|
| O(1) | 1.677 | 1.803 | 1.803 |
| O(2) | 1.707 | 1.665 | |
| | 2.393 | 0.260 | 1.925 |
| O(3) | 1.935 | 0.900 | |
| | 1.970 | 0.818 | |
| | 2.219 | 0.417 | 2.135 |
| $V_{.13}Mo_{.87}$ | 1.677 | 1.803 | |
| | 1.707 | 1.665 | |
| | 1.935 | 0.900 | |
| | 1.970 | 0.818 | |
| | 2.219 | 0.417 | |
| | 2.393 | 0.260 | 5.863 |

the tunnel of approximately 3.3 Å, assuming an ionic radius for oxygen of 1.35 Å. The open nature of this structure is reflected by the large molar volume compared to the other known polymorphs of $MoO_3$. As shown in Table V, the volume of the hexagonal structure, per formula unit of "$MoO_3$", is 18% larger than the thermodynamically stable $\alpha$ form, and 12% larger than the $ReO_3$-related $\beta$ and $\beta'$ phases. It is to be expected that the increased porosity of the hexagonal phase will lead to a wide range of ion-insertion properties, and our preliminary experi-

ments indicate monovalent ions can readily be inserted into the structure.

Finally it is interesting to compare the lattice parameters and volume of the open h-$MoO_3$ structure with those that contain large stabilizing cations in the tunnels, i.e., $A_{0.13}V_{0.13}Mo_{0.87}O_3$ ($A$ = K, Rb, and Cs). The lattice parameters of the empty tunnel structure represent, in essence, the "equilibrium" lattice dimensions for the structure. As Table VI indicates, the $a$ lattice parameter of open h-$MoO_3$ falls between those for Rb and Cs. Apparently both K and Rb are somewhat too small for the tunnels and force the framework to contract; on the other hand, Cs is slightly too large and is accommodated by a small framework expansion.

## Conclusions

A series of lithium–hydronium isomorphs of vanadium-stabilized hexagonal $MoO_3$, $\{Li_xH_{.13-x}\}(V_{.13}Mo_{.87})O_3 \cdot 0.26H_2O$, can be directly precipitated from acidic Li–V–Mo solutions within a narrow range of pH, composition, and temperature. At room temperature these precipitates undergo a rapid ion-exchange reaction in 0.5 $M$ HCl to give the pure protonic form of hexagonal $MoO_3$, $H_{.13}(V_{.13}Mo_{.87})O_3 \cdot 0.26H_2O$. Complete dehydration of this solid acid yields the open form of hexagonal $MoO_3$, $(V_{.13}Mo_{.87})O_{2.935}$, which is stable up to 460°C. Powder neutron

### TABLE V

Comparison of the "Porosity" of Different Polymorphs of $MoO_3$

| Structure | $\alpha$-$MoO_3$ | $\beta$-$MoO_3$ | $\beta'$-$MoO_3$ | $(V_{.13}Mo_{.87})O_{2.935}$ |
|---|---|---|---|---|
| $a$ (Å) | 3.963 | 7.122 | 7.4245 | 10.593 |
| $b$ (Å) | 13.856 | 5.374 | 7.4783 | 10.593 |
| $c$ (Å) | 3.697 | 5.565 | 7.6897 | 3.694 |
| $b$ (°) | 90 | 91.88 | 90.090 | 120 |
| $V_{unit\ cell}$ (Å$^3$) | 203.0 | 212.9 | 427.0 | 359.0 |
| $z$ | 4 | 4 | 8 | 6 |
| $V_{per\ MoO_3}$ (Å$^3$) | 50.8 | 53.2 | 53.4 | 59.8 |
| Reference | (1) | (2) | (5) | this work |

TABLE VI

LATTICE PARAMETERS OF VANADIUM-STABILIZED H-MoO₃, $A_{.13}(V_{.13}Mo_{.87})O_3$

| $A$ | $a$ (Å)$^a$ | $c$ (Å)$^a$ | $V_{unit\ cell}$ (Å$^3$) | $r_A$ (Å) |
|---|---|---|---|---|
| K | 10.481 | 3.701 | 352.09 | 1.38 |
| Rb | 10.523 | 3.698 | 354.63 | 1.52 |
| Cs | 10.617 | 3.694 | 360.60 | 1.67 |
| $(V_{.13}Mo_{.87})O_{2.935}$ | 10.593 | 3.694 | 359.01 | — |

$^a$ See Ref. (14).

diffraction has been used to confirm that the one-dimensional channels in the structure are empty and that the anion vacancies are located at the unshared oxygen positions.

## Acknowledgments

## References

1. L. KIHLBORG, Ark. Kemi 21, 357 (1963).
2. E. M. McCARRON III; J. Chem. Soc. Chem. Commun. 4, 336 (1986).
3. G. SVENSSON AND L. KIHLBORG, React. Solids 3, 33 (1987).
4. F. HARB, B. GERAND, G. NOWOGROCKI, AND M. FIGLARZ, Solid State Ionics 32/33, 84 (1989).
5. J. B. PARISE, E. M. McCARRON III, AND A. W. SLEIGHT, Mat. Res. Bull. 22, 803 (1987).
6. N. SOTANI, Bull. Chem. Soc. Jpn. 48, 1820 (1975).
7. J. M. TATIBOUET AND J. E. GERMAIN, C. R. Seances Acad. Sci. Ser. C 290, 321 (1980).
8. J. M. TATIBOUET AND J. E. GERMAIN, J. Catal. 72, 375 (1981).
9. J. C. VOLTA AND J. L. PORTEFAIX, Appl. Catal. 18, 1 (1985).
10. J. E. GERMAIN, in "Adsorption and Catalysis on Oxide Surfaces" (M. Che and G. C. Bond, Eds.), p. 355, Elsevier, Amsterdam (1985).
11. E. M. McCARRON III, D. M. THOMAS, AND J. C. CALABRESE, Inorg. Chem. 26, 371 (1987).
12. B. KREBS AND I. PAULAT-BOSCHEN, Acta Crystallogr. Sect. B 32, 1697 (1976).
13. N. A. CAIGER, S. CROUCH-BAKER, P. G. DICKENS, AND G. S. JAMES, J. Solid State Chem. 67, 369 (1987).
14. B. DARRIET AND J. GALY, J. Solid State Chem. 8, 189 (1973).
15. I. P. OLENKOVA, L. M. PLYASOVA, AND S. D. KIRIK, React. Kinet. Catal. Lett 16, 81 (1981).
16. T. P. FEIST AND P. K. DAVIES, in "Chemistry of Electronic Ceramic Materials, Proceedings of an International Conference Held in Jackson Hole, WY" (P. K. Davies and R. S. Roth, Eds.), p. 163, NIST, SP 804 (1991).
17. T. P. FEIST AND P. K. DAVIES, Chem. Mater. 3, 1011 (1991).
18. M. T. POPE, "Heteropoly and Isopoly Oxometalates," Springer-Verlag, Berlin/Heidelberg, 1983.
19. Y. HU AND P. K. DAVIES, unpublished results.
20. B. GERAND, G. NOWOGROCKI, J. GUENOT, AND M. FIGLARZ, J. Solid State Chem. 29, 429 (1979).
21. I. D. BROWN, in "Structure and Bonding in Crystals," (M. O'Keeffe and A. Navrotsky, Eds.), Vol. II, p. 1 Academic Press, New York (1981).
22. N. E. BRESE AND M. O'KEEFFE, Acta Crystallogr. Sect. B 47, 192 (1991).